



# Discovery of two skin-derived dermaseptins and design of a TAT-fusion analogue with broad-spectrum antimicrobial activity and low cytotoxicity on healthy cells

Haohao Zhu<sup>1,2,\*</sup>, Xiyan Ding<sup>1,2,\*</sup>, Wei Li<sup>1</sup>, Tulin Lu<sup>1</sup>, Chengbang Ma<sup>2</sup>, Xinpeng Xi<sup>2</sup>, Lei Wang<sup>2</sup>, Mei Zhou<sup>2</sup>, Roberta Burden<sup>2</sup> and Tianbao Chen<sup>2</sup>

<sup>1</sup>School of Pharmacy, Nanjing University of Chinese Medicine, Nanjing, China

<sup>2</sup>School of Pharmacy, The Queen's University Belfast, Belfast, United Kingdom

\*These authors contributed equally to this work.

## ABSTRACT

Two novel peptides belonging to the dermaseptin family, namely DRS-CA-1 and DRS-DU-1, were encoded from cDNA libraries derived from the skin secretions of *Phyllomedusa camba* and *Callimedusa (Phyllomedusa) duellmani*. Both natural peptides are highly-conserved and exhibited high potency against wild-type Gram-positive, Gram-negative bacteria, yeast and antibiotic-resistant bacteria (MRSA and *Pseudomonas aeruginosa*) (MICs 4–8  $\mu$ M) with no obvious hemolytic activity. Collectively these results suggest that both peptides may have potential as novel antibiotics. Additionally, DRS-DU-1 exhibited selective cytotoxicity to tumor cells. The truncated analogue, DP-1 and TAT-fused DP-1 (namely DP-2) were subsequently synthesised. It showed that DP-1 had low antimicrobial activity, no hemolytic and cytotoxicity to tumor cells. However, DP-2 possessed strong antimicrobial activity and the similar selective, no obvious hemolytic activity and cytotoxicity on normal human cells, but enhanced cytotoxicity to tumor cells of DRS-DU-1. These findings indicate that the N-terminus of the dermaseptins may contribute to their bioactivity, and that addition of the TAT peptide can improve biological activity. The results provide a new insight for designing novel peptide-based antimicrobial or anticancer agents with low hemolytic activity and cytotoxicity.

Submitted 7 March 2018  
Accepted 24 August 2018  
Published 19 September 2018

Corresponding authors  
Wei Li, [liwaii@126.com](mailto:liwaii@126.com)  
Chengbang Ma, [c.ma@qub.ac.uk](mailto:c.ma@qub.ac.uk)

Academic editor  
Marta Kostrouchova

Additional Information and  
Declarations can be found on  
page 13

DOI 10.7717/peerj.5635

© Copyright  
2018 Zhu et al.

Distributed under  
Creative Commons CC-BY 4.0

OPEN ACCESS

**Subjects** Biochemistry, Bioengineering, Molecular Biology, Synthetic Biology

**Keywords** Molecular cloning, Skin secretion, Dermaseptin, Antimicrobial peptide, Cell viability.

## INTRODUCTION

Due to the lack of efficacy of current antibiotics against increasing numbers of drug-resistant pathogens, antimicrobial peptides are considered as the compounds with the most potential to take over traditional antibiotics against drug-resistant bacteria (*Li et al., 2012*). Peptides with antimicrobial and antifungal activity have vital roles in the innate immune system, which constitutes the first line of defense against a wide range of animal-invading pathogens (*Shi et al., 2014; Chen et al., 2006*). The skin secretions of frogs from all around the world

have been proven to be a valuable source of these antimicrobial peptides, with more than one thousand antimicrobial peptides with significant different structural features having been extracted and characterized (Erspamer et al., 1985; Azevedo-Calderon et al., 2011).

Dermaseptins are the largest family of antimicrobial peptides identified from the skin secretions of *Phyllomedusa* species. Although they show some differences in their lengths, they are clearly related, given that almost all members are K-rich polycationic peptides, with a tryptophan residue at position 3 and a highly-conserved motif in the central or C-terminal region (Nicolas & El Amri, 2009). Peptides belonging to the dermaseptin family normally have two apparent separated lobes of hydrophobicity and a positively-charged electrostatic surface, resulting in the coil-to-helix transition upon association with lipid bilayers (Chen, Tang & Shaw, 2003; Wang et al., 2008). The dermaseptins usually have lytic activity and are lethal against Gram-positive and Gram-negative bacteria, fungi and protozoa at micromolar concentrations (Shin et al., 1994). Despite dermaseptins having identical amino acid sequences, they show significant differences in their efficiency and cytolytic activities, which was thought to be independent of the envelope structure of bacteria (Rivas, Luque-Ortega & Andreu, 2009; Navon-Venezia et al., 2002; Huang et al., 2017). The antimicrobial potency of dermaseptin S3 (from *Phyllomedusa sauvagii*) was not affected after shortening its chain length, the truncated N-terminal domain still retained complete or even better lytic activity against some bacteria (Kustanovich et al., 2002). Besides, the truncated analogues, such as K<sub>4</sub>-S4(1-13)a and K<sub>4</sub>-S4(1-15)a from dermaseptin S4, exhibited even lower cytotoxic effect on erythrocytes than the parent peptide (Shepherd, Vogel & Tieleman, 2003; Feder, Dagan & Mor, 2000a).

Although most dermaseptins were discovered by their antimicrobial activity, they were still reported to be effective against the cancer cells. Dermaseptin B2 and B3 (from *Phyllomedusa bicolor*) exhibited potent anti-proliferative effect on PC-3 cells, and dermaseptin B2 inhibited the tumor growth of PC-3 cells *in vivo* (Van Zoggel et al., 2012b; Van Zoggel et al., 2012a). The further study showed that dermaseptin B2 could interact with glycosaminoglycan (GAGs) on the surface of PC-3 for cell internalization (Santos et al., 2017). Besides, dermaseptin PH (from *Pithecopus hypochondrialis*), PD1 and PD2 (from *Pachymedusa dacnicolor*) were reported to exhibit cytotoxicity against several human cancer cell lines (Huang et al., 2007; Shi et al., 2016).

In this study, we report two novel dermaseptins, namely DRS-CA-1 and DRS-DU-1, that were discovered by molecular cloning from cDNA libraries derived from the skin secretion of *Phyllomedusa camba* and *Callimedusa (Phyllomedusa) duellmani*. The mature peptides were subsequently synthesized by solid-phase peptide synthesis and purified for functional assays. In addition, two analogues were designed based on the results to study the potential cytotoxicity to tumor cells of dermaseptins.

## MATERIALS AND METHODS

### Specimen biodata and secretion harvesting

Adult specimens of *P. camba* and *C. duellmani* were obtained from commercial sources (PeruBiotech E.I.R.L., Lima, Peru). Before harvesting the skin secretion, all frogs were

cultivated in the purpose-designed amphibian facility for at least four months, conditioned at 20–25 °C with 12h/12 h light/dark cycle and fed with multivitamin-loaded crickets three times per week. The defensive skin secretions were produced by stimulation the glands on the skin surface of frogs with gentle transdermal electrical stimulation (6V DC; 4 ms pulse-width; 50 Hz) through platinum electrodes for two periods of 20 s duration. The study was performed according to the guidelines in the UK Animal (Scientific Procedures) Act 1986, project license PPL 2694, issued by the Department of Health, Social Services and Public Safety, Northern Ireland. Procedures had been vetted by the IACUC of Queen's University Belfast, and approved on 1st March, 2011.

### **Molecular cloning of the dermaseptin peptide precursor-encoding cDNAs**

Five milligrams of crude lyophilized skin secretions were used to obtain polyadenylated mRNA using the Dynabeads<sup>®</sup> mRNA DIRECT<sup>™</sup> kit (DynaL Biotech Ltd, Wirral, UK). cDNA library construction and primary cDNA amplification were performed with a BD SMART<sup>™</sup> RACE cDNA amplification kit (BD Biosciences, UK) to give full-length prepro-peptide nucleic acid sequence data. The degenerate sense primer (S1; 5'-ACTTTCYGAWTTTRYAAGMCCAAABATG-3') (Y = C + T, W = A + T, R = A + G, M = A + C, B = T + C + G) applied in the RACE reactions were designed according to the highly conserved domain of the 5'-untranslated region of dermaseptin cDNAs from *Phyllomedusa* species. RACE products were subjected to gel analysis, and the detected bands were purified and cloned using the pGEM<sup>®</sup>-T Easy vector system (Promega, Madison, WI, USA). The sequences were obtained from an ABI 3100 automated capillary sequencer.

### **Reverse phase HPLC fractionation of crude skin secretion and amino-acid sequence analysis of relevant peptides**

A further five milligrams of lyophilised skin secretion were dissolved in 0.5 ml of 0.05% (v/v) trifluoroacetic acid (TFA)/water and clarified by centrifugation. The clear supernatant was subjected to reverse-phase HPLC on an analytical column (Jupiter C-5, 250 mm × 10 mm; Phenomenex, Cheshire, UK), eluted with a 0–80% linear gradient of acetonitrile containing 0.05% (v/v) TFA in 240 min at a flow rate of 1 ml/min. Absorbance was monitored at 214 nm. The peptide mapping of two natural occurring peptides was conducted using MS/MS fragmentation sequencing against the cDNA encoding peptide precursors by LCQ electrospray ion-trap mass spectrometer (Thermo Fisher Scientific, Waltham, MA, USA).

### **Solid-Phase Peptide Synthesis**

Both the natural peptides and the analogs were chemically synthesized through the solid-phase method with standard Rink amide resin and Fluorenylmethoxycarbonyl (Fmoc) chemistry in a PS4 automated solid-phase synthesizer (Protein Technologies, Inc, Tucson, AZ, USA). After cleavage from the resin and the protecting groups, the crude peptides were purified and analyzed by reverse-phase HPLC and MALDI-TOF mass spectrometry.

## Secondary structure and physicochemical properties prediction of the peptides

I-TASSER webserver was applied to predict the secondary structures of the synthetic peptides (Roy, Kucukural & Zhang, 2010). Physicochemical properties of the peptides were predicted by Heliquest and the helical wheel plots of the secondary structures were obtained from the helical wheel projections (Gautier et al., 2008).

In addition, circular dichroism (CD) analyses were performed on the JASCO J815 Spectropolarimeter (JASCO Inc., Easton, MD, USA). The measure range of each sample was 190–260 nm, and the parameters were set as follows: 0.5 nm data pitch, 1 nm bandwidth and 200 nm/min scanning speed. The peptide samples were prepared with 10 mM ammonium acetate buffer and 50% trifluoroethanol (TFE) in 10 mM ammonium acetate buffer at a concentration of 100  $\mu$ M. The percentage of the  $\alpha$ -helix structure was predicted by BESTSEL online software (Micsonai et al., 2015).

## Antimicrobial assays

Gram-positive bacteria *Staphylococcus aureus* (NCTC10788), methicillin-resistant *Staphylococcus aureus* (MRSA) (NCTC12493), and *Enterococcus faecalis* (NCTC 12697); Gram-negative bacteria *Escherichia coli* (NCTC 10418), *Pseudomonas aeruginosa* (ATCC 27853), and *Klebsiella pneumoniae* (ATCC 43816), and the yeast *Candida albicans* (NCYC 1467) were chosen to determine the antimicrobial activities of synthesized peptides through evaluating the minimum inhibitory concentration (MIC) and minimum bactericidal concentration (MBC). The microorganisms were cultured in Muller Hinton Broth (MHB, Oxoid, UK) medium and incubated in the orbital incubator (Stuart, UK) at 37 °C overnight and then sub-cultured in a pre-warmed MHB medium until the bacteria reached their respective logarithmic growth phases. The sub-cultured suspension was diluted with fresh medium to a concentration of  $5 \times 10^5$  colony forming units (CFU)/ml. The peptides with different concentrations were prepared in DMSO from 512  $\mu$ M to 1  $\mu$ M. The MICs were determined in 96-well microtiter plates by mixing the peptides with bacteria, and 1% DMSO in MHB was applied as the negative control. After an incubation of 20 h, the growth of microorganisms was detected at a wavelength of 550 nm in a Synergy HT plate reader (Biolise BioTek EL808, Winooski, VT, USA). The MICs were determined as the lowest concentration of peptide where no apparent growth of the microorganism was detectable. Subsequently, 10  $\mu$ l of solution in each well was spotted on the Mueller Hinton Agar (MHA) plates. The MBC values were determined as the lowest concentration of peptide where no growth was observed on the MHA plate.

## Hemolysis assay

Fresh defibrinated horse blood (TCS Biosciences Ltd, Buckingham, UK) was used to perform the hemolysis assay. The serum and erythrocytes were separated by centrifugation and the erythrocytes were collected and washed with PBS. Peptides in concentration gradients were incubated with 4% (v/v) erythrocyte suspension at 37 °C for 2 h. 1% DMSO and triton X-100 (Sigma Aldrich, St. Louis, MO, USA) was used as the negative and positive control, respectively. After centrifugation, 100  $\mu$ l supernatants were transferred to a 96-well

plate and absorbance measured at 550 nm using a Synergy HT plate reader (BioTec, Auburn, CA, USA). Peptide concentration causing 50% hemolysis of the red bloods cells ( $HC_{50}$ ) was calculated [ $\% \text{ haemolysis} = (A - A_0) / (AX - A_0) \times 100$ , where 'A' is absorbance with peptides of different concentrations, 'A0' is absorbance with negative controls and 'AX' is absorbance with positive controls] to determine the hemolysis activities. The therapeutic index (TI) was calculated as  $HC_{50}$  divided by the geometric mean of the MIC values against relevant bacteria.

### Cell lines and cell culture

Human prostate carcinoma cell line PC-3 (ATCC-CRL-1435), non-small cell lung cancer cell line H157 (ATCC-CRL-5802), breast cancer cell line MDA-MB-435s (ATCC-HTB-129), neuronal glioblastoma cell line U251MG (ECACC-09063001) and breast cancer non-tumorigenic mammary gland cell line MCF-7 (ATCC-HTB-22) were utilized to screen the cytotoxicity of synthetic peptides. PC-3 and H157 cell lines were cultured in RPMI-1640 medium (Invitrogen, Paisley, UK), and the other cell lines were cultured with Dulbecco's Modified Eagle's medium (DMEM) (Sigma, St. Louis, MO, USA). Culture media was supplemented with 10% fetal bovine serum (FBS) (Sigma, Welwyn Garden City, UK) and 1% penicillin streptomycin solution (Sigma, UK). The human mammary epithelial cell line, HMEC-1 (ATCC-CRL-3243) was used to evaluate the cytotoxicity of the synthetic peptides against normal human cells, and cultured with MCDB131 medium (Gibco, Paisley, UK) with 10% FBS, 10ng/ml EGF, 10mM L-Glutamine and 1% penicillin streptomycin. The selected cell lines were resuscitated and transferred into a 75 cm<sup>2</sup> culture flask, and then incubated at 37 °C atmosphere containing 5% CO<sub>2</sub>.

### Assessment of antiproliferative activity with the MTT assay

MTT cell viability assay was used to assess the proliferation and viability of different cell lines. After cell quantification, the cell suspension was mixed with pre-warmed medium to the final concentration of  $5 \times 10^3$  cells in 96-well plates. After treating with serum-free medium, various concentrations of peptides were added and incubated for 24 h, 1% DMSO in related culture media was treated as the negative control. A total of 10  $\mu$ l of MTT solution (5 mg/ml) (Sigma, Welwyn Garden City, UK) was added to each well and incubated for 4 h. Supernatants were removed by syringe and 100  $\mu$ l of DMSO was used to resuspend the insoluble purple formazan crystals. The absorbance of each well was measured at 570 nm with the Synergy HT plate reader (BioTek, Winooski, VT, USA), data were analysed to obtain the mean and standard error of responses. The dose-response curves were constructed using a "best-fit" algorithm and then the half maximal inhibitory concentrations ( $IC_{50}$ ) were calculated through the data analysis package provided in GraphPad Prism 6 (GraphPad Software, USA).

## RESULTS

### Identification of two dermaseptins from their skin secretion and bioinformatic analyses of novel peptides

Two novel peptides, namely DRS-CA-1 and DRS-DU-1, were encoded from two different cDNA libraries derived from *P. camba* and *C. duellmani*, which were the first dermaseptin

A)

**M A F L K K S L F L V L F L G L V** ·  
 1 ATGGCTTTCT TGAAGAAATC TCTTTTCCTT GACTATTCC TTGGATTGGT  
 TACCGAAAGA ACTTCTTTAG AGAAAAGGAA CATGATAAGG AACCTAACCA  
 · **S L S I C E E E K R E N E E K E N** ·  
 51 TTCTCTTTCT ATCTGTGAAG AAGAGAAAAG AGAAAATGAA GAGAAAGAAA  
 AAGAGAAAGA TAGACACTTC TTCTCTTTTC TCTTTTACTT CTCTTTCTTT  
 · **Q E D D E Q S E E K R A L W K D**  
 101 ATCAAGAAGA TGATGAGCAA AGTGAAGAGA AGAGAGCTCT GTGGAAAGAT  
 TAGTTCTTCT ACTACTCGTT TCACTTCTCT TCTCTCGAGA CACCTTTCTA  
 · **L L K N V G K A A G K A V L N K V** ·  
 151 TTATTAATAA ATGTAGGGAA AGCTGCAGGA AAAGCGGTTT TAAATAAAGT  
 AATAATTTTT TACATCCCTT TCGACGTCCT TTTTCGCCAA ATTTATTTCA  
 · **T D M V N Q G E Q** \*  
 201 TACTGATATG GTAAATCAAG GAGAGCAATA AAGTTAAGAA AATGTAAATT  
 ATGACTATAC CATTTAGTTC CTCTCGTTAT TTCAATTCTT TTACATTTAA  
 251 TCATAACTCT AAGGAGCACA ATTATCAATA ATTGTAGGCA AACTTATATT  
 AGTATTGAGA TTCCTCGTGT TAATAGTTAT TAACATCCGT TTGAATATAA  
 301 AAAGCATATT GAACAAAAA AAAAAAAAAA AAAAAAAAAA  
 TTTTCGTATAA CTTGTTTTTT TTTTTTTTTT TTTTTTTTTT

B)

**M A F I K K S L F L V L F L G L V** ·  
 1 ATGGCTTTCA TTAAGAAATC TCTTTTCCTT GACTATTCC TTGGATTGGT  
 TACCGAAAGT AATTCCTTAG AGAAAAGGAA CATGATAAGG AACCTAACCA  
 · **S L S I C E E E K R E N E E E N N** ·  
 51 TTCCCTTTCC ATCTGTGAAG AAGAGAAAAG AGAAAATGAA GAAGAAAATA  
 AAGGGAAAGG TAGACACTTC TTCTCTTTTC TCTTTTACTT CTTCTTTTAT  
 · **Q E D D E Q S E E K R A L W K S**  
 101 ATCAAGAAGA TGATGAGCAA AGTGAAGAGA AGAGAGCTCT GTGGAAATCT  
 TAGTTCTTCT ACTACTCGTT TCACTTCTCT TCTCTCGAGA CACCTTTAGA  
 · **L L K N V G K A A G K A A L N A V** ·  
 151 TTATTAATAA ATGTAGGGAA AGCTGCAGGA AAAGCGGCTT TAAATGCAGT  
 AATAATTTTT TACATCCCTT TCGACGTCCT TTTTCGCCAA ATTTACGTCA  
 · **T D M V N Q G E Q** \*  
 201 TACTGATATG GTAAATCAAG GAGAGCAATA AAGTTAAGAA AATGTAAATC  
 ATGACTATAC CATTTAGTTC CTCTCGTTAT TTCAATTCTT TTACATTTAG  
 251 AAATTGCTCT AAGGAGCACA AATTAATCAA TCAATTGTTA ACTTAGCTTA  
 TTTAACGAGA TTCCTCGTGT TTAATTAGTT AGTTAACAAT TGAATCGAAT  
 301 TATTAAGCA TATTGAACCA AAAAAAAAAA AAAAAAAAAA  
 ATAATTTTCGT ATAATTGGT TTTTTTTTTT TTTTTTTTTT

**Figure 1** Translated amino acid sequence of the open-reading frame and nucleotide sequence of cloned cDNA encoding the biosynthetic precursor of DRS-CA-1 (A) from *Callimedusa (Phyllomedusa) camba* and DRS-DU-1 (B) from *Phyllomedusa duellmani*. The putative signal peptides are marked with double line, mature peptides are marked with single line and stop codons are indicated by an asterisk.

Full-size [DOI: 10.7717/peerj.5635/fig-1](https://doi.org/10.7717/peerj.5635/fig-1)

discovered from respective frog species. The nucleotide and translated open-reading frame consisting of 76 amino acid sequences are shown in Fig. 1. Both contain 16-residue signal peptide regions, followed by a 16-residue Glu-rich acidic peptide spacer and 28-residue mature peptide with typical dermaseptin sequence, connected by two -KR- propeptide convertase processing sites. The extension (-GEQ-) was also observed, of which G acted

**Table 1** The predicted physicochemical properties and secondary structure of DRS-CA-1, DRS- DU-1, DP-1, and DP-2. Data from physico-chemical property prediction.

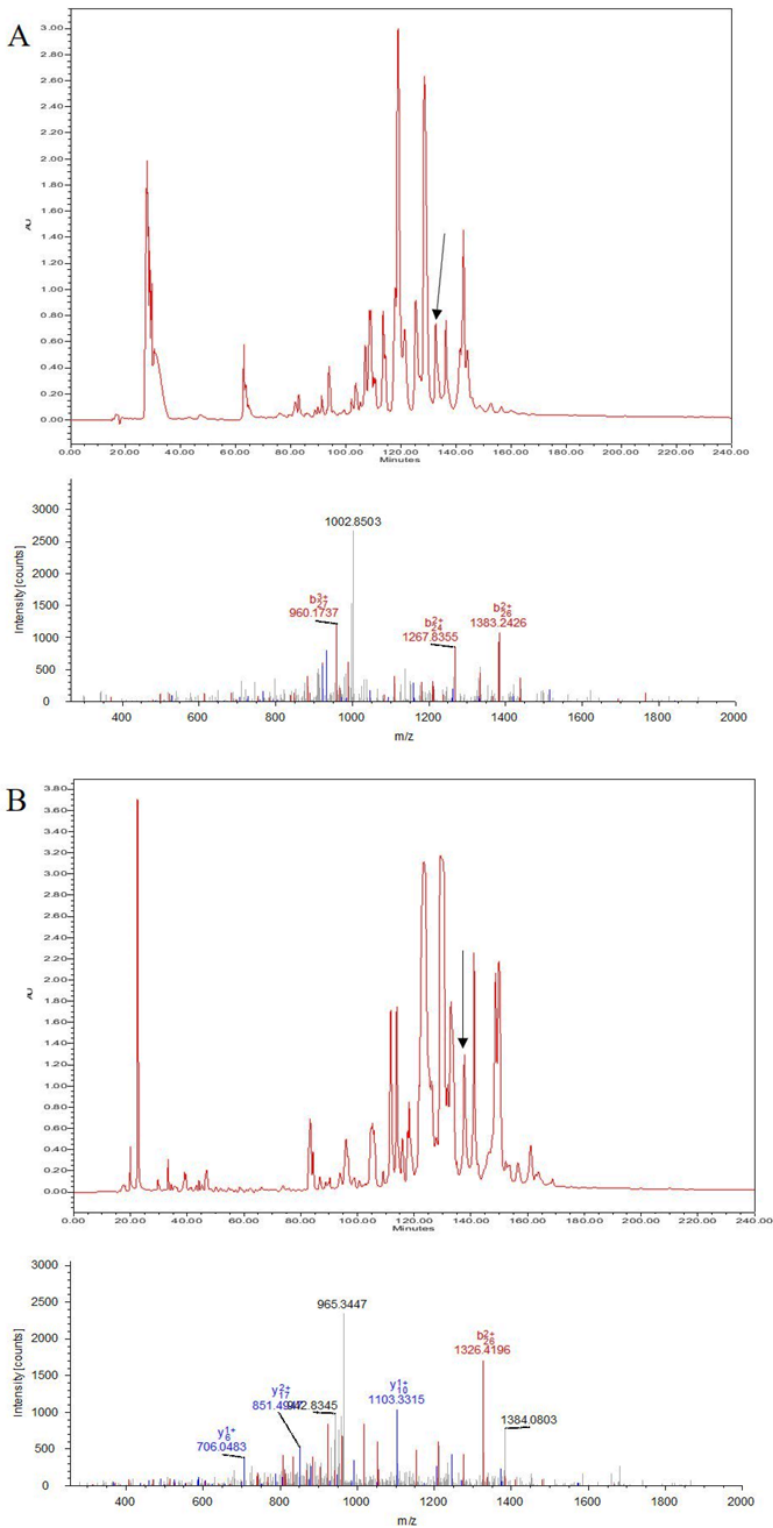
Peptides	Sequence	$\alpha$ -Helicity (%)	Hydrophobicity (H)	Hydrophobic moment ( $\mu$ H)	Net charge
DRS-CA-1	ALWKDLLKNVGKAAGKAVLNKVTDMVNQ.NH <sub>2</sub>	25.3	0.291	0.263	+3
DRS-DU-1	ALWKSLLKNVGKAAGKAALNAVTDNVNQ.NH <sub>2</sub>	27.9	0.331	0.255	+3
DP-1	ALWKSLLKNVGKA.NH <sub>2</sub>	16.1	0.429	0.645	+3
DP-2	GRKKRRQRRRGALWKSLLKNVGKA.NH <sub>2</sub>	11.4	-0.112	0.358	+11

as a donor for C-terminal amidation of mature peptides. LC-MS analysis confirmed the presence of DRS-CA-1 and DRS-DU-1 in the skin secretion of *P. camba* and *C. duellmani*, respectively, possessing the post-translational modification of C-terminal amidation (Figs. 2A and 2B). Alignment of the full length nucleic acid sequences and the open-reading frame sequences of the two cloned precursors are shown in Fig. 3. Both nucleotide and amino acid sequences demonstrated high degree of similarity (92%) between two biosynthetic precursors. Specifically, there was only one residue different in the signal peptides and three residues different in the mature peptides between the two moieties. A BLAST search in the Nonredundant Protein Sequence Database showed that several dermaseptins isolated from different frog species share a high degree of identity of amino acid sequences with the two dermaseptins identified herein and their open-reading frame sequences also exhibited remarkable similarities in the acidic peptides (Fig. 3). The cDNA sequences of two dermaseptin precursors have been deposited in the GenBank Database under the accession codes [MF955846](#) and [MF955847](#).

### Design, synthesis, physicochemical properties and secondary structure prediction of peptides and their analogues

Considering the length of dermaseptin, N-terminal of 13-mer truncated mimetic peptide, DP-1, was designed following the previous study (Feder, Dagan & Mor, 2000b). In the meantime, the TAT (GRKKRRQRRR) peptide was introduced at the N-terminal of DP-1 to improve its cell-penetration ability, namely DP-2. A Gly was added as a linker between TAT and DP-1. Both dermaseptins and the designed analogues were successfully synthesized and purified.

The predicted physicochemical properties and secondary structures of the peptides are shown in Table 1 and Fig. 4, respectively. Both natural peptides had 3 positive net charges and possessed  $\alpha$ -helical secondary structure. Additionally, the calculated  $\alpha$ -helicity of the natural peptides based on the CD spectra is 23.5% and 27.9%, respectively. However, DP-1 had lower degree of helicity as 16.1% though it had the same net charges and relatively higher hydrophobicity and hydrophobic moment. Whilst, DP-2 contained the lowest helical content of 11.4%. Helical wheel plots of four peptides are shown in Fig. 4C. The two natural peptides formed the hydrophobic face, which are associated with antimicrobial activity of peptides. However, both DP-1 and DP-2 revealed no uninterrupted hydrophobic face.



#1	b(1+)	b(2+)	b(3+)	Seq.	y(1+)	y(2+)	y(3+)	#2
1	72.044	36.526	24.686	A				28
2	185.128	93.068	62.381	L	2952.6817	1476.8445	984.8988	27
3	371.208	186.108	124.407	W	2839.5976	1420.3025	947.2041	26
4	499.303	250.155	167.106	K	2653.5183	1327.2628	885.1776	25
5	614.330	307.668	205.448	D	2525.4234	1263.2153	842.4793	24
6	727.414	364.211	243.143	L	2410.3964	1205.7018	804.1370	23
7	840.498	420.753	280.837	L	2297.3123	1149.1598	766.4423	22
8	968.593	484.800	323.536	K	2184.2283	1092.6178	728.7476	21
9	1082.636	541.822	361.550	N	2056.1333	1028.5703	686.0493	20
10	1181.704	591.356	394.573	V	1942.0904	971.5488	648.0350	19
11	1238.726	619.866	413.580	G	1843.0219	922.0146	615.0122	18
12	1366.821	683.914	456.278	K	1786.0005	893.5039	596.0050	17
13	1437.858	719.433	479.957	A	1657.9055	829.4564	553.3067	16
14	1508.895	754.951	503.636	A	1586.8684	793.9378	529.6276	15
15	1565.916	783.462	522.644	G	1515.8313	758.4193	505.9486	14
16	1694.011	847.509	565.342	K	1458.8098	729.9085	486.9415	13
17	1765.048	883.028	589.021	A	1330.7148	665.8611	444.2431	12
18	1864.117	932.562	622.044	V	1259.6777	630.3425	420.5641	11
19	1977.201	989.104	659.738	L	1160.6093	580.8083	387.5413	10
20	2091.244	1046.126	697.753	N	1047.5252	524.2662	349.8466	9
21	2219.339	1110.173	740.451	K	933.4823	467.2448	311.8323	8
22	2318.407	1159.707	773.474	V	805.3873	403.1973	269.1340	7
23	2419.455	1210.231	807.156	T	706.3189	353.6631	236.1112	6
24	2534.482	1267.745	845.499	D	605.2712	303.1392	202.4286	5
25	2665.522	1333.265	889.179	M	490.2443	245.6258	164.0863	4
26	2764.591	1382.799	922.202	V	359.2038	180.1055	120.4061	3
27	2878.634	1439.820	960.216	N	260.1353	130.5713	87.3833	2
28				Q- Amidated	146.0924	73.5498	49.3690	1

#1	b(1+)	b(2+)	b(3+)	Seq.	y(1+)	y(2+)	y(3+)	#2
1	72.044	36.526	24.686	A				28
2	185.128	93.068	62.381	L	2839.598	1420.302	947.204	27
3	371.208	186.108	124.407	W	2726.514	1363.760	909.509	26
4	499.303	250.155	167.106	K	2540.434	1270.721	847.483	25
5	586.335	293.671	196.116	S	2412.339	1206.673	804.785	24
6	699.419	350.213	233.811	L	2325.307	1163.157	775.774	23
7	812.503	406.755	271.506	L	2212.223	1106.615	738.079	22
8	940.598	470.803	314.204	K	2099.139	1050.073	700.385	21
9	1054.641	527.824	352.218	N	1971.044	986.026	657.686	20
10	1153.709	577.358	385.241	V	1857.001	929.004	619.672	19
11	1210.731	605.869	404.248	G	1757.933	879.470	586.649	18
12	1338.826	669.916	446.947	K	1700.911	850.959	567.642	17
13	1409.863	705.435	470.626	A	1572.816	786.912	524.944	16
14	1480.900	740.954	494.305	A	1501.779	751.393	501.265	15
15	1537.921	769.464	513.312	G	1430.742	715.875	477.586	14
16	1666.016	833.512	556.010	K	1373.721	687.364	458.578	13
17	1737.053	869.030	579.689	A	1245.626	623.316	415.880	12
18	1808.091	904.549	603.368	A	1174.589	587.798	392.201	11
19	1921.175	961.091	641.063	L	1103.551	552.279	368.522	10
20	2035.218	1018.112	679.077	N	990.467	495.737	330.827	9
21	2106.255	1053.631	702.756	A	876.424	438.716	292.813	8
22	2205.323	1103.165	735.779	V	805.387	403.197	269.134	7
23	2306.371	1153.689	769.462	T	706.319	353.663	236.111	6
24	2421.398	1211.203	807.804	D	605.271	303.139	202.429	5
25	2552.438	1276.723	851.484	M	490.244	245.626	164.086	4
26	2651.507	1326.257	884.507	V	359.204	180.106	120.406	3
27	2765.550	1383.278	922.521	N	260.135	130.571	87.383	2
28				Q- Amidated	146.092	73.550	49.369	1

**Figure 2** Identification of (A) DRS-CA-1 and (B) DRS-DU-1 from the corresponding skin secretions. The retention times of DRS-CA-1 and DRS-DU-1 are indicated by arrows in the respective HPLC chromatograms. The spectra and the tables beside demonstrate the peptide mapping using the SEQUEST algorithm.

Full-size DOI: 10.7717/peerj.5635/fig-2



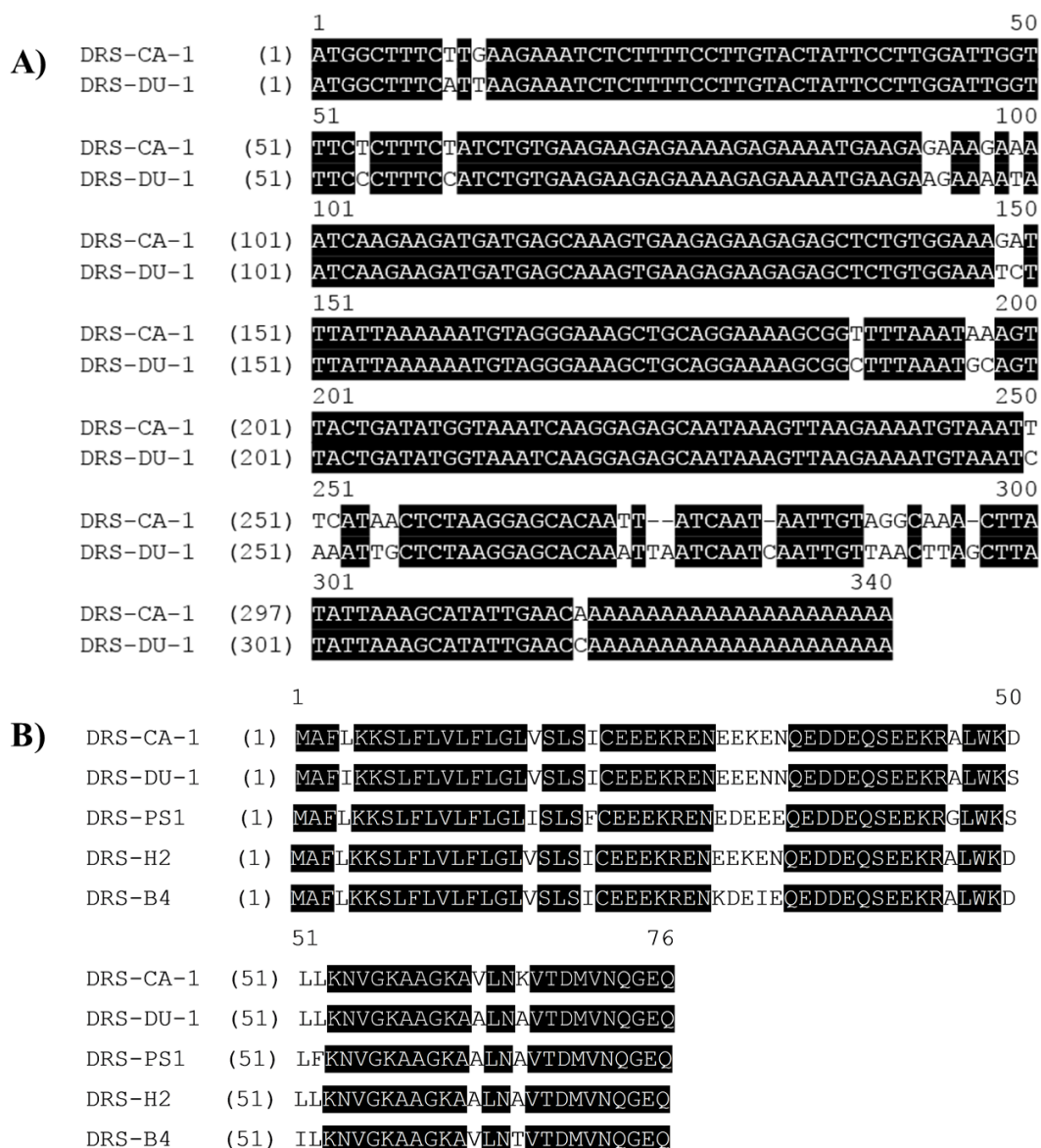


**Figure 3** (A) Alignment of nucleotide sequences of cloned cDNAs encoding the biosynthetic precursors of DRS-CA-1 and DRS-DU-1. (B) Alignment of open-reading frame sequences of DRS-CA-1, DRS-DU-1 and other dermaseptin peptides characterized from other species. (DRS-PS1 from *P. sauvagii* (accession number P24302), DRS-H2 from *P. hypochondrialis* (accession number P84597) and DRS-B4 from *P. bicolor* (accession number P81486)). Conserved amino acid residues are shaded in black.

Full-size  DOI: 10.7717/peerj.5635/fig-3

## Antimicrobial and hemolytic activities

The MIC, MBC and HC<sub>50</sub> values of all the peptides obtained from antimicrobial and hemolysis assays are summarized in Table 2. The two natural peptides, DRS-CA-1 and DRS-DU-1, showed the same MIC values (4 μM) against *S. aureus* and *E. coli* and *C. albicans*. DRS-DU-1 was twofold more potent against MRSA, *E. faecalis*, *K. pneumoniae* and *P. aeruginosa* than DRS-CA-1. The MBC values of two natural peptides against seven tested

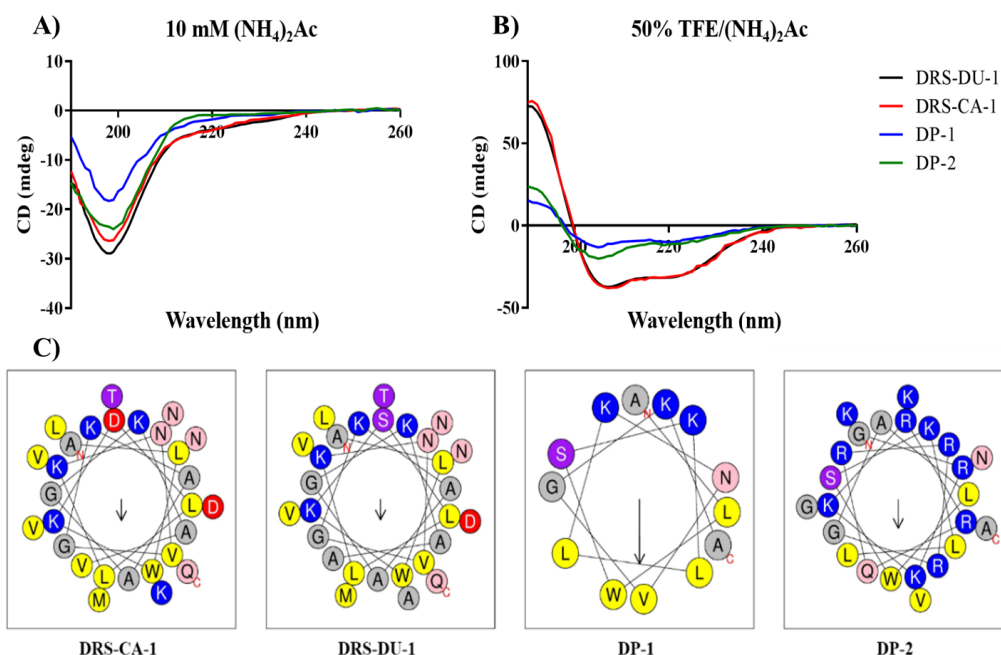


**Figure 4** CD spectra of the four peptides (100  $\mu$ M) in 10 mM ammonium acetate buffer (A) and 50% TFE ammonium acetate buffer (B). Helical wheel projections (Gautier et al., 2008) of peptides (C), with the arrow indicated the direction of the hydrophobic moments. All the peptides exhibit random coil structure in the aqueous solution while they are able to form  $\alpha$ -helical structure in the membrane-mimetic environment. The hydrophobic (yellow), hydrophilic (purple), positively-charged (blue), negatively-charged (red), amide (pink) and small (grey) residues are presented.

Full-size DOI: 10.7717/peerj.5635/fig-4

**Table 2** Antimicrobial (MIC and MBC) and hemolytic (HC<sub>50</sub>) activity, and relative safety (TI) of DRS-CA-1, DRS-DU-1, DP-1, and DP-2. Data represent the mean of  $\geq 3$  determinations.

Strains	MIC/MBC ( $\mu$ M)			
	DRS-CA-1	DRS-DU-1	DP-1	DP-2
<i>S. aureus</i>	4/16	4/16	64/128	8/8
MRSA	8/32	4/16	128/128	16/16
<i>E. faecalis</i>	128/256	64/128	256/>512	32/128
<i>E. coli</i>	4/16	4/16	64/128	4/8
<i>P. aeruginosa</i>	8/32	4/16	128/256	8/16
<i>K. pneumoniae</i>	8/128	4/64	128/>512	32/256
<i>C. albicans</i>	4/16	4/16	32/64	4/8
Horse Erythrocytes (HC <sub>50</sub> )	114.7	216.6	>512	>512
TI (overall)	21.73	54.15	13.93	147.13

microorganisms were two or four-fold higher than respective MICs. No obvious hemolysis activity was detected at the MIC or MBC concentrations except against *E. faecalis*.

The two designed peptides also exhibited broad spectrum antimicrobial activities against the seven tested microorganisms, though the potency of DP-1 was much lower. However, the antimicrobial activities of DP-2 were restored comparing to DP-1. Additionally, the antimicrobial potency of DP-2 on *E. faecalis* was higher than the natural peptides.

**Table 3** IC<sub>50</sub> of DRS-CA-1, DRS-DU-1, DP-1, and DP-2 against tested human cancer cells and human normal cell. The cytotoxicity of dermaseptin B2 (DRSB2), dermaseptin PH (DRSPH), dermaseptin PD1 (DRSPD1) and dermaseptin PD2 (DRSPD2) obtained from published data were shown in the table for comparison.

Cell lines	IC <sub>50</sub> (μM)							
	DRS-CA-1	DRS-DU-1	DP-1	DP-2	DRSB2	DRSPH	DRSPD1	DRSPD2
HMEC-1	>100	53.75	>100	>100	NA	4.85	36.35	27.28
H157	>100	8.43	>100	3.21	NA	2.01	NA	6.43
PC-3	>100	21.6	>100	6.75	2.17	11.8	NA	3.17
MDA-MB-435s	>100	>100	>100	>100	>10	9.94	NA	NA
U251MG	>100	>100	>100	>100	NA	2.36	15.08	13.43
MCF-7	>100	>100	>100	>100	NA	0.69	NA	NA

**Notes.**

NA, not tested.

### Anti-Proliferative Effects of the Peptides

The anti-proliferative IC<sub>50</sub> values of the natural peptides and designed peptides determined by MTT assay are summarized in Table 3. DRS-CA-1 and DP-1 were found to possess no obvious anti-proliferative activity against all five human cancer cell lines and normal human cells. DRS-DU-1 had selective activity against H157 and PC-3 cells, with IC<sub>50</sub> values of 8.43 μM and 21.6 μM, respectively. Although DP-1 had no activity against all cancer cell lines, the activity of DP-2 was improved considerably, with the IC<sub>50</sub> values of 3.21 μM and 6.75 μM against H157 and PC-3 cells respectively. In addition, the cytotoxicity against normal human cell line (HMEC-1) of DRS-DU-1 (IC<sub>50</sub> of 53.75) was eliminated. The IC<sub>50</sub> values of DP-1 and DP-2 against HMEC-1 are both greater than 100 μM.

## DISCUSSION

Many bacteria have developed resistance against conventional antibiotics that has pressed researchers to discover novel antibacterial agents (Neu, 1992). In recent years, antimicrobial peptides isolated from amphibian skin secretions have become a hot topic in both academic and industrial drug discovery research. It is believed that most antimicrobial peptides act on the cell membrane, and can distinguish target from host cells through differences in fluidity and the negative charge density of their membranes. Such properties make it unlikely for the bacterial pathogens to become resistant to antimicrobial peptides (Yeaman & Yount, 2003). However, studies reported that the resistance of bacteria to AMPs has emerged recently, by producing positively-charged molecules on the membrane, and pumping AMPs out of cells (Joo, Fu & Otto, 2016; Andersson, Hughes & Kubicek-Sutherland, 2016). Therefore, discovery and design more effective antimicrobial peptide seems to be urgent and important.

In this study, we aimed to discover novel bioactive peptides from two rarely studied species of the Phyllomedusidae family, *P. camba* and *C. duellmani*. As a result, two novel dermaseptin peptides were successfully identified. The nucleotide and translated open-reading frame sequences of the peptides have almost identical signal peptide sequences,

the same prepropeptide processing site and amino donor. Furthermore, they differ by only two amino acids in the acidic peptide sequence and three residues in the mature peptides. Through the NCBI-BLAST search, it is interesting to note that the two novel precursors not only exhibit high homology to the different types of antimicrobial peptides from the Phyllomedusidae frogs, but also to other antimicrobial peptides from the Hylidae tree frogs. More than 80% identity were shared in the signal peptide domain between the two dermaseptins precursors and the antimicrobial peptides derived from the Hylidae frogs, including dermatoxin, medusin, caerin, cruzioseptin and phylloseptin ([Chen et al., 2005](#); [Gao et al., 2017](#); [Gao et al., 2016](#); [Pukala et al., 2006](#); [Proano-Bolanos et al., 2016](#)). This is the reason of the evolution from the ancestors that were selected by the surroundings to form diverse bioactive peptides for their unique defense system ([Vanhoye et al., 2003](#)).

DRS-CA-1 and DRS-DU-1 exhibited strong antimicrobial activity against Gram-positive and Gram-negative bacteria and fungi with no obvious hemolytic activity, and almost the same proportion of polar residues and nonpolar residues as well as the  $\alpha$ -helical structure. The positive net charge of antimicrobial peptides had been widely accepted as the key factor to help the peptide combine with the negatively-charge bacteria cell surface. Besides, the hydrophobic surface of the peptides in the  $\alpha$ -helical structure could ensure the peptides permeabilize the membrane. Although resistance against antimicrobial peptides have emerged, this bacterial-killing mechanism of dermaseptin is distinctly different from conventional antibiotics, which makes it promising in relation to overcoming antibiotic resistance problems ([Lee, Hall & Aguilar, 2016](#)). Comparing to the two most famous dermaseptins, dermaseptin B2 and S4, both natural peptides demonstrated potent antimicrobial activities, though dermaseptin B2 showed strongly inhibitory effect on *E. coli* ([Kustanovich et al., 2002](#); [Joanne et al., 2009](#)). As the studies indicated, more cationicity of dermaseptin could improve the antimicrobial activity as well as the spectrum, which is consistent with study of introduce of Lys at positions 7 and 14 of dermaseptin S4 that remarkably increased the antimicrobial activity against *P. aeruginosa* ([Jiang et al., 2014](#)). Additionally, the study of truncated analogues demonstrated that the integrity of N-terminus is essential for possessing the antimicrobial activity while reducing the haemolysis within certain degree ([Kustanovich et al., 2002](#)). Therefore, we assumed that the 13-mer N-terminal truncated analogue, DP-1, will retain the antimicrobial potency of the patent peptides, but will become less hemolytic. Although the DP-1 had the same ratio of polar/nonpolar residues, higher hydrophobic moment and same positive net charge, it might not form the proper  $\alpha$ -helical structure resulting in significant reduction of its antimicrobial activity against all microorganisms. The data is different comparing to the previous study of the structure–activity relationship of dermaseptin S4 ([Kustanovich et al., 2002](#)), in which peptides with same physico-chemical properties usually have similar potency. This phenomenon indicates the importance of peptide's secondary structure in designing short antimicrobial peptides. Interestingly, when the TAT peptide was added, its antimicrobial activity was enhanced remarkably with reduced hemolytic activity. Considering their structural difference, this can be explained by the increased positive charges, which can enhance the interaction with the negative charge bacterial membranes. However, research has revealed that a high positive charge could lead to an increased

hemolytic activity and a loss of antimicrobial potency (Dathe *et al.*, 2001), which is not corresponding with the results. We hypothesize that TAT peptide associated the attachment to the surface of bacteria, which subsequently allow the helical region of DP-1 segment to permeabilize the cell membrane.

Although dermaseptin has been reported to induce necrosis in PC-3 cancer cells, there are researches showing that dermaseptin could enter the cytoplasm and the nucleus (Santos *et al.*, 2017; Auvynet *et al.*, 2006). We also noticed that the sensitivity to dermaseptin varies due to different type of cancer cells. On the sensitive cells, PC-3, researches indicated that the internalization mechanism may be initiated through the interaction with negatively-charged glycosaminoglycan (GAGs) (Santos *et al.*, 2017). Therefore, the disappearance of cytotoxic activity of DP-1 could be the shorter sequence and lower helicity that decreases the permeability against cell membrane, as well as the affinity to cancer cells for the GAGs mediated internalization. However, the restore of cytotoxicity activity of DP-2 suggests that fused-TAT improved the affinity of DP-2 to the cell membrane and initiated the interaction with GAGs.

On the other hand, the cytotoxicity of antimicrobial peptides on normal mammalian cells is mostly associated with the hydrophobicity and helicity of those peptides. The typical membrane lytic peptide, melittin, possesses an average helicity of 70% at membrane interfaces (Andersson *et al.*, 2013). When reviewing the researches of different dermaseptins, we found that the increase of helicity not only improved antimicrobial and cytotoxic effect, but also increased the cytotoxicity on both normal cell lines and erythrocytes [12, 20]. For instance, that dermaseptin-PH showed a  $\alpha$ -helicity of 35% may be related to the high degree of cytotoxicity on HMEC-1 (Huang *et al.*, 2017). The presence of cytotoxicity on both cancer cells and HMEC-1 of DRS-DU1 than DRS-CA1 could be also speculated by the higher  $\alpha$ -helicity. Additionally, researches of truncated dermaseptin analogues also indicates that the integrity of  $\alpha$ -helix and hydrophobic domain is important for the bio-activity of dermaseptin (Auvynet *et al.*, 2006). Moreover, that the effects of DP-2 on HMEC-1 and erythrocytes were remained mild is consistent with the hypothesis of GAGs involved internalization as proportion of GAGs is larger than which is on the healthy cells.

In summary, two novel dermaseptins were deduced from the skin secretion of *P. camba* and *C. duellmani* with broad-spectrum antimicrobial activity even against drug-resistant strains (MRSA and *Pseudomonas aeruginosa*) with low hemolytic activity, which makes them promising in the treatment of multidrug-resistant bacteria. This study revealed the importance of the TAT peptide in the design of antimicrobial or anti-proliferative cancer agents through enhancing their biological function. All of these provide a new idea for designing novel peptide-based antimicrobial or anti-proliferative agents.

## ADDITIONAL INFORMATION AND DECLARATIONS

### Funding

Haohao Zhu and Xiyan Ding received a scholarship from the China Scholarship Council. This work was supported by the National Natural Science Foundation of China (No.

81573304), Jiangsu Collaborative Innovation Center of Chinese Medicinal Resources Industrialization (No. ZDXM-2-1) and the Priority Academic Program Development of Jiangsu Higher Education Institutions. The funders had no role in study design, data collection and analysis, decision to publish, or preparation of the manuscript.

### **Grant Disclosures**

The following grant information was disclosed by the authors:

National Natural Science Foundation of China: 81573304.

Jiangsu Collaborative Innovation Center of Chinese Medicinal Resources Industrialization: ZDXM-2-1.

Priority Academic Program Development of Jiangsu Higher Education Institutions.

### **Competing Interests**

The authors declare there are no competing interests.

### **Author Contributions**

- Haohao Zhu performed the experiments, analyzed the data, authored or reviewed drafts of the paper.
- Xiyan Ding performed the experiments, analyzed the data.
- Wei Li contributed reagents/materials/analysis tools, prepared figures and/or tables, approved the final draft.
- Tulin Lu contributed reagents/materials/analysis tools, prepared figures and/or tables.
- Chengbang Ma performed the experiments, analyzed the data, prepared figures and/or tables.
- Xinpeng Xi contributed reagents/materials/analysis tools, authored or reviewed drafts of the paper, approved the final draft.
- Lei Wang and Mei Zhou conceived and designed the experiments.
- Roberta Burden authored or reviewed drafts of the paper.
- Tianbao Chen conceived and designed the experiments, approved the final draft.

### **Animal Ethics**

The following information was supplied relating to ethical approvals (i.e., approving body and any reference numbers):

The study was performed according to the guidelines in the UK Animal (Scientific Procedures) Act 1986, project license PPL 2694, issued by the Department of Health, Social Services and Public Safety, Northern Ireland. Procedures had been vetted by the IACUC of Queen's University Belfast, and approved on 1st March, 2011.

### **DNA Deposition**

The following information was supplied regarding the deposition of DNA sequences:

The cDNA sequences of two dermaseptin precursors have been deposited in the GenBank Database under the accession codes [MF955846](#) and [MF955847](#).

### **Data Availability**

The following information was supplied regarding data availability:

The raw data are provided in the [Supplemental File](#).

## Supplemental Information

Supplemental information for this article can be found online at <http://dx.doi.org/10.7717/peerj.5635#supplemental-information>.

## REFERENCES

- Andersson DL, Hughes D, Kubicek-Sutherland JZ. 2016. Mechanisms and consequences of bacterial resistance to antimicrobial peptides. *Drug Resistance Updates* 26:43–57 DOI 10.1016/j.drug.2016.04.002.
- Andersson M, Ulmschneider JP, Ulmschneider MB, White SH. 2013. Conformational states of melittin at a bilayer interface. *Biophysical Journal* 104:L12–L14 DOI 10.1016/j.bpj.2013.02.006.
- Auvynet C, Seddiki N, Dunia I, Nicolas P, Amiche M, Lacombe C. 2006. Post-translational amino acid racemization in the frog skin peptide deltorphin I in the secretion granules of cutaneous serous glands. *European Journal of Cell Biology* 85:25–34 DOI 10.1016/j.ejcb.2005.09.022.
- Azevedo-Calderon L, Sliva A, Ciancaglini P, Stabeli RG. 2011. Antimicrobial peptides from Phyllomedusa frogs: from biomolecular diversity to potential nanotechnologic medical applications. *Amino Acids* 40:29–49 DOI 10.1007/s00726-010-0622-3.
- Chen T, Li L, Zhou M, Rao P, Walker B, Shaw C. 2006. Amphibian skin peptides and their corresponding cDNAs from single lyophilized secretion samples: identification of novel brevinins from three species of Chinese frogs. *Peptides* 27:42–48 DOI 10.1016/j.peptides.2005.06.024.
- Chen T, Tang L, Shaw C. 2003. Identification of three novel *Phyllomedusa sauvagei* dermaseptins (sVI–sVIII) by cloning from a skin secretion-derived cDNA library. *Regulatory Peptides* 116:139–146 DOI 10.1016/j.regpep.2003.08.001.
- Chen T, Walker B, Zhou M, Shaw CC. 2005. Dermatoxin and phylloxin from the waxy monkey frog, *Phyllomedusa sauvagei*: cloning of precursor cDNAs and structural characterization from lyophilized skin secretion. *Regulatory Peptides* 129:103–108 DOI 10.1016/j.regpep.2005.01.017.
- Dathe M, Nikolenko H, Meyer J, Beyermann M, Bienert M. 2001. Optimization of the antimicrobial activity of magainin peptides by modification of charge. *FEBS Letters* 501:146–150 DOI 10.1016/S0014-5793(01)02648-5.
- Erspamer V, Melchiorri P, Erspamer GF, Montecucchi PC, De Castiglione R. 1985. Phyllomedusa skin: a huge factory and store-house of a variety of active peptides. *Peptides* 6:7–12.
- Feder R, Dagan A, Mor A. 2000a. Structure-activity relationship study of antimicrobial dermaseptin S4 showing the consequences of peptide oligomerization on selective cytotoxicity. *Journal of Biological Chemistry* 275:4230–4238 DOI 10.1074/jbc.275.6.4230.

- Feder R, Dagan A, Mor A. 2000b.** Structure-activity relationship study of antimicrobial dermaseptin S4 showing the consequences of peptide oligomerization on selective cytotoxicity. *Journal of Biological Chemistry* **275**:4230–4238 DOI [10.1074/jbc.275.6.4230](https://doi.org/10.1074/jbc.275.6.4230).
- Gao Y, Wu D, Wang L, Lin C, Ma C, Xi X, Shaw C. 2017.** Targeted Modification of a novel amphibian antimicrobial peptide from *Phyllomedusa tarsius* to enhance its activity against MRSA and microbial biofilm. *Frontiers in Microbiology* **8**:Article 628.
- Gao Y, Wu D, Xi X, Wu Y, Ma C, Zhou M, Shaw C. 2016.** Identification and characterisation of the antimicrobial peptide, phylloseptin-PT, from the skin secretion of *Phyllomedusa tarsius*, and comparison of activity with designed, cationicity-enhanced analogues and diastereomers. *Molecules* **21**:Article 1667 DOI [10.3390/molecules21121667](https://doi.org/10.3390/molecules21121667).
- Gautier R, Douguet D, Antony B, Drin G. 2008.** HELIQUEST: a web server to screen sequences with specific  $\alpha$ -helical properties. *Bioinformatics* **24**:2101–2102 DOI [10.1093/bioinformatics/btn392](https://doi.org/10.1093/bioinformatics/btn392).
- Huang L, Chen D, Wang L, Lin C, Ma C, Xi X, Chen T, Shaw C, Zhou M. 2017.** Dermaseptin-PH: a novel peptide with antimicrobial and anticancer activities from the skin secretion of the south American orange-legged leaf frog, *Pithecopus (Phyllomedusa) hypochondrialis*. *Molecules* **22**:Article 1805 DOI [10.3390/molecules22101805](https://doi.org/10.3390/molecules22101805).
- Huang L, Chen D, Wang L, Lin C, Ma C, Xi X, Zhou M. 2007.** Dermaseptin-PH: a novel peptide with antimicrobial and anticancer activities from the skin secretion of the South American Orange-legged leaf frog, *Pithecopus (Phyllomedusa) hypochondrialis*. *Molecules* **22**:Article 1805.
- Jiang Z, Vasil AI, Vasil ML, Hodges RS. 2014.** “Specificity determinants” improve therapeutic indices of two antimicrobial peptides piscidin 1 and dermaseptin S4 against the gram-negative pathogens *Acinetobacter baumannii* and *Pseudomonas aeruginosa*. *Pharmaceuticals* **7**:366–391 DOI [10.3390/ph7040366](https://doi.org/10.3390/ph7040366).
- Joanne P, Galanth C, Goasdoué N, Nicolas P, Sagan S, Lavielle S, Alves ID. 2009.** Lipid reorganization induced by membrane-active peptides probed using differential scanning calorimetry. *Biochimica et Biophysica Acta (BBA)—Biomembranes* **1788**:1772–1781 DOI [10.1016/j.bbamem.2009.05.001](https://doi.org/10.1016/j.bbamem.2009.05.001).
- Joo HS, Fu CI, Otto M. 2016.** Bacterial strategies of resistance to antimicrobial peptides. *Philosophical Transactions of the Royal B: Biological Sciences* **371**:Article 20150292 DOI [10.1098/rstb.2015.0292](https://doi.org/10.1098/rstb.2015.0292).
- Kustanovich I, Shalev DE, Mikhlin M, Gaidukov L, Mor A. 2002.** Structural requirements for potent versus selective cytotoxicity for antimicrobial dermaseptin S4 derivatives. *Journal of Biological Chemistry* **277**:16941–16951 DOI [10.1074/jbc.M111071200](https://doi.org/10.1074/jbc.M111071200).
- Lee TH, Hall KN, Aguilar MI. 2016.** Antimicrobial peptide structure and mechanism of action: a focus on the role of membrane structure. *Current Topics in Medicinal Chemistry* **16**:25–39.



- Li R, Wang H, Jiang Y, Yu Y, Wang L, Zhou M, Chen T, Shaw C. 2012.** A novel Kazal-type trypsin inhibitor from the skin secretion of the Central American red-eyed leaf frog, *Agalychnis callidryas*. *Biochimie* **94**:1376–1381 DOI [10.1016/j.biochi.2012.03.009](https://doi.org/10.1016/j.biochi.2012.03.009).
- Micsonai A, Wien F, Kernya L, Lee YH, Goto Y, Réfrégiers M, Kardos J. 2015.** Accurate secondary structure prediction and fold recognition for circular dichroism spectroscopy. *Proceedings of the National Academy of Sciences of the United States of America* **112**:E3095–E3103.
- Navon-Venezia S, Feder R, Gaidukov L, Carmeli Y, Mor A. 2002.** Antibacterial properties of dermaseptin S4 derivatives with in vivo activity. *Antimicrobial Agents and Chemotherapy* **46**:689–694 DOI [10.1128/AAC.46.3.689-694.2002](https://doi.org/10.1128/AAC.46.3.689-694.2002).
- Neu HC. 1992.** The crisis in antibiotic resistance. *Science* **257**:1064–1074 DOI [10.1126/science.257.5073.1064](https://doi.org/10.1126/science.257.5073.1064).
- Nicolas P, El Amri C. 2009.** The dermaseptin superfamily: a gene-based combinatorial library of antimicrobial peptides. *Biochimica et Biophysica Acta/General Subjects* **1788**:1537–1550.
- Proano-Bolanos C, Zhou M, Wang L, Coloma LA, Chen T, Shaw C. 2016.** Peptidomic approach identifies cruzioseptins, a new family of potent antimicrobial peptides in the splendid leaf frog, *Cruziophyla calcarifer*. *Journal of Proteomics* **146**:1–13 DOI [10.1016/j.jprot.2016.06.017](https://doi.org/10.1016/j.jprot.2016.06.017).
- Pukala TL, Bertozzi T, Donnellan SC, Bowie JH, Surinya KH, Liu Y, Tyler MJ. 2006.** Host-defence peptide profiles of the skin secretions of interspecific hybrid tree frogs and their parents, female *Litoria splendida* and male *Litoria caerulea*. *The FEBS Journal* **273**:3511–3519 DOI [10.1111/j.1742-4658.2006.05358.x](https://doi.org/10.1111/j.1742-4658.2006.05358.x).
- Rivas L, Luque-Ortega JR, Andreu D. 2009.** Amphibian antimicrobial peptides and Protozoa: lessons from parasites. *BBA-Biomembranes* **1788**:1570–1581 DOI [10.1016/j.bbamem.2008.11.002](https://doi.org/10.1016/j.bbamem.2008.11.002).
- Roy A, Kucukural A, Zhang Y. 2010.** I-TASSER: a unified platform for automated protein structure and function prediction. *Nature Protocols* **5**:725–738 DOI [10.1038/nprot.2010.5](https://doi.org/10.1038/nprot.2010.5).
- Santos CD, Hamadat S, Saux KL, Newton C, Mazouni M, Zargarian L, Amiche M. 2017.** Studies of the antitumor mechanism of action of dermaseptin B2, a multifunctional cationic antimicrobial peptide, reveal a partial implication of cell surface glycosaminoglycans. *PLOS ONE* **12**:e0182926 DOI [10.1371/journal.pone.0182926](https://doi.org/10.1371/journal.pone.0182926).
- Shepherd CM, Vogel HJ, Tieleman DP. 2003.** Interactions of the designed antimicrobial peptide MB21 and truncated dermaseptin S3 with lipid bilayers: molecular-dynamics simulations. *Biochemical Journal* **370**:233–243 DOI [10.1042/bj20021255](https://doi.org/10.1042/bj20021255).
- Shi D, Hou X, Wang L, Gao Y, Wu D, Xi X, Shaw C. 2016.** Two novel dermaseptin-like antimicrobial peptides with anticancer activities from the skin secretion of *Pachymedusa dactinicolor*. *Toxins* **8**:Article 144 DOI [10.3390/toxins8050144](https://doi.org/10.3390/toxins8050144).
- Shi D, Luo Y, Du Q, Wang L, Zhou M, Ma J, Chen T, Shaw C. 2014.** A novel bradykinin-related dodecapeptide (RVALPPGFFTPLR) from the skin secretion of the fujian large-headed frog (*Limnonectes fujianensis*) exhibiting unusual structural and functional features. *Toxins* **6**:2886–2898 DOI [10.3390/toxins6102886](https://doi.org/10.3390/toxins6102886).

- Shin Y, Moni RW, Lueders JE, Daly JW. 1994.** Effects of the amphiphilic peptides mastoparan and adenoregulin on receptor binding, G proteins, phosphoinositide breakdown, cyclic AMP generation, and calcium influx. *Cellular and Molecular Neurobiology* **14**:133–157 DOI [10.1007/BF02090781](https://doi.org/10.1007/BF02090781).
- Van Zoggel H, Carpentier G, Santos CD, Hamma-Kourbali Y, Courty J, Amiche M, Delbé J. 2012a.** Antitumor and angiostatic activities of the antimicrobial peptide dermaseptin B2. *PLOS ONE* **7**:e44351 DOI [10.1371/journal.pone.0044351](https://doi.org/10.1371/journal.pone.0044351).
- Van Zoggel H, Hamma-Kourbali Y, Galanth C, Ladram A, Nicolas P, Courty J, Delbé J. 2012b.** Antitumor and angiostatic peptides from frog skin secretions. *Amino Acids* **42**:385–395 DOI [10.1007/s00726-010-0815-9](https://doi.org/10.1007/s00726-010-0815-9).
- Vanhoye D, Bruston F, Nicolas P, Amiche M. 2003.** Antimicrobial peptides from hylid and ranin frogs originated from a 150-million-year-old ancestral precursor with a conserved signal peptide but a hypermutable antimicrobial domain. *The FEBS Journal* **270**:2068–2081.
- Wang L, Zhou M, McClelland A, Reilly A, Chen T, Gagliardo R, Walker B, Shaw C. 2008.** Novel dermaseptin, adenoregulin and caerin homologs from the Central American red-eyed leaf frog, *Agalychnis callidryas*, revealed by functional peptidomics of defensive skin secretion. *Biochimie* **90**:1435–1441 DOI [10.1016/j.biochi.2008.04.016](https://doi.org/10.1016/j.biochi.2008.04.016).
- Yeaman MR, Yount NY. 2003.** Mechanisms of antimicrobial peptide action and resistance. *Pharmacological Reviews* **55**:27–55 DOI [10.1124/pr.55.1.2](https://doi.org/10.1124/pr.55.1.2).